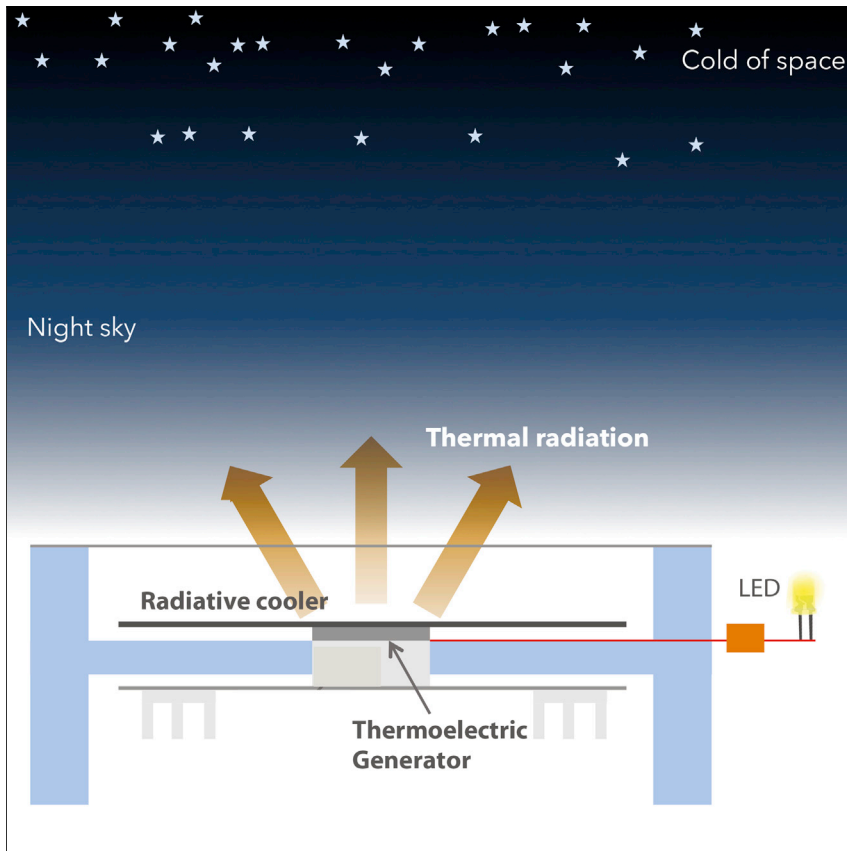


Report

Generating Light from Darkness



Night-time power generation analogous to photovoltaics would be an enabling capability for applications such as lighting and wireless sensors. We demonstrate a low-cost power generation device based on thermoelectric generators where the cold side radiates heat to the cold of space by facing the night sky. The power generated is sufficient to maintain a LED lit at night, enabling battery-free off-grid lighting. Device performance is validated with a model, and pathways to improved performance are highlighted.

Aaswath P. Raman, Wei Li,
Shanhui Fan

aaswath@ucla.edu (A.P.R.)
shanhui@stanford.edu (S.F.)

HIGHLIGHTS

A thermoelectric generator is built whose cold side radiates heat to the sky

Night-time power generation of 25 mW/m^2 is demonstrated, sufficient for a LED

Pathways to performance $> 0.5 \text{ W/m}^2$ using existing commodity components exist

This approach is immediately practical for lighting and off-grid sensors

Report

Generating Light from Darkness

Aaswath P. Raman,^{1,3,*} Wei Li,² and Shanhui Fan^{2,*}

SUMMARY

A large fraction of the world's population still lacks access to electricity, particularly at night when photovoltaic systems no longer operate. The ability to generate electricity at night could be a fundamentally enabling capability for a wide range of applications, including lighting and low-power sensors. Here, we demonstrate a low-cost strategy to harness the cold of space through radiative cooling to generate electricity with an off-the-shelf thermoelectric generator. Unlike traditional thermoelectric generators, our device couples the cold side of the thermoelectric module to a sky-facing surface that radiates heat to the cold of space and has its warm side heated by the surrounding air, enabling electricity generation at night. We experimentally demonstrate 25 mW/m² of power generation and validate a model that accurately captures the device's performance. Further, we show that the device can directly power a light emitting diode, thereby generating light from the darkness of space itself.

INTRODUCTION

Generating electricity through renewable means has motivated a wide array of fundamental and applied science and engineering over the past century. While photovoltaics has offered a viable commercial path to achieving this goal both at grid and small scale during the day, achieving small-scale, distributed renewable power generation at night without storage remains challenging. This paucity of options at night poses a particular challenge for the 1.3 billion people worldwide that lack reliable access to electricity; a population that represents a quarter of the developing world's population.¹ Demand for electricity among such rural populations in the developing world is surging, with three applications in particular driving interest: cell phone charging, cooking, and lighting.^{2,3} Lighting solutions for resource-constrained, off-grid communities have drawn much global interest with a range of approaches implemented.⁴ Solar lights have made progress at this task but, as lighting demand peaks at night, require the coupling of photovoltaic or solar thermal modules to a battery, driving up costs. A modular way to generate electricity at night without the need for storage would thus have direct and significant implications for lighting applications. Beyond lighting, a broad range of low-power off-grid sensors could also benefit from a modular power generation source at night.

Thermodynamically, for any energy conversion process to produce useful work, for example, electricity, there must be a hot source and a cold sink. Most renewable approaches to electricity generation, including photovoltaics and solar thermal systems, rely on using the Sun as the hot source and the ambient surroundings of Earth as a cold sink. At night, however, no such ubiquitous and easily accessible hot source exists to drive a heat engine. On the other hand, there does exist a ubiquitous cold sink that has to-date been largely ignored: the cold of outer space. Using the ambient air surrounding Earth's surface instead as the heat source and space as the cold sink, then, would allow one to drive a new kind of night-time heat engine and generate electricity at night. Remarkably, accessing the coldness of space is

Context & Scale

Reliable energy access remains a challenge, particularly in off-grid regions throughout the world. While solar cells have enabled distributed power generation during the day, no comparable alternative exists at night. In this report, we demonstrate a low-cost, modular mechanism of renewably generating meaningful amounts of electricity at night by harnessing the cold darkness of space. We use a passive cooling mechanism known as radiative sky cooling to maintain the cold side of a thermoelectric generator several degrees below ambient. The surrounding air heats the warm side of the thermoelectric generator, with the ensuing temperature difference converted into usable electricity. We highlight pathways to improving performance from a demonstrated 25 mW/m² to 0.5 W/m². Finally, we demonstrate that even with the low-cost implementation demonstration here, enough power is produced to light a LED: generating light from darkness.

indeed possible through radiative heat transfer between a sky-facing surface and outer space. A significant fraction of thermal radiation from a sky-facing surface can pass through the atmosphere and reach outer space, enabling passive radiative cooling of the surface to well below the ambient air temperature. Early work on radiative cooling focused on evaluating materials for their ability to cool passively at night.^{5–10} More recently, sub-ambient radiative cooling during the day has also been demonstrated through a range of materials strategies including photonic structures,^{11–13} metamaterials,¹⁴ and novel synthesis methods.¹⁵ On an energy system level, radiative cooling has been evaluated for a range of implementations,^{16,17} including for building-scale cooling applications^{18–20} and in conjunction with solar thermal collectors.^{21,22}

While the ability to passively maintain a surface below ambient air temperature is useful, for applications such as lighting one needs to convert the temperature difference between the ambient and cold surface into usable electricity. One direct path to doing this in a modular and tractable way is to use a thermoelectric generator. Thermoelectric generators have attracted significant attention in the past two decades, with one line of inquiry seeking to use them to recover usable power from waste heat escaping a small-scale thermal system, such as that from a fire or stove.²³ Considerable research is also ongoing to improve thermoelectric generator efficiency^{24,25} with a view toward both off-grid power generation and waste heat recovery at industrial scales. However, the vast majority of approaches using thermoelectrics for night-time power generation require an active input of heat.

Previous theoretical works derived the limits for generating electricity from Earth's net infrared emissions to space.^{26,27} In this paper, we experimentally demonstrate a simple, low-cost way of generating electricity at night based on a thermoelectric module that generates enough electricity to passively power a light emitting diode (LED) at night. This system is entirely passive, i.e., with no active power input, and is constructed in a low-cost modular fashion. We characterize the system's performance under a clear night sky under varying loads. We then show that the system's performance can be effectively modeled using knowledge of the thermoelectric module's properties, the air temperature, and the atmospheric properties in the mid-infrared window where the sky is transparent. Finally, we show that the electricity generated is enough to power a LED—thus, we generate light from darkness.

RESULTS

Experimental Demonstration

To demonstrate the potential of night-time power generation using radiative heat exchange with space, we built and tested a low-cost thermoelectric generator where the cold side was coupled to a simple black emitter ($\epsilon \sim 0.95$) facing the sky and the hot side heated by the ambient by natural convection. The device, schematically shown in Figure 1A consists of a polystyrene enclosure covered in aluminized mylar to minimize thermal radiation from the enclosure and an infrared-transparent wind cover made from 12.5 μm -thick low-density polyethylene previously used in radiative cooling implementations.^{7,13} The thermal emitter consists of 200 mm aluminum disk painted with a commercial black paint ($\epsilon \sim 0.95$). The disk is adhered with heat transfer paste to the cold side of a commercial thermoelectric module (Marlowe TG12-4, $ZT = 0.71$). The hot side of the module is coupled to a small aluminum block adhered to a 200 mm aluminum disk with multiple fins outside the enclosure. The entire device sat on a table approximately 1m above roof level. The completed device is shown in Figure 1B in rooftop testing.

¹Department of Materials Science and Engineering, University of California, Los Angeles, Los Angeles, CA 90024, USA

²Ginzton Laboratory, Stanford University, Stanford, CA 94305, USA

³Lead Contact

*Correspondence: aaswath@ucla.edu (A.P.R.), shanhui@stanford.edu (S.F.)

<https://doi.org/10.1016/j.joule.2019.08.009>

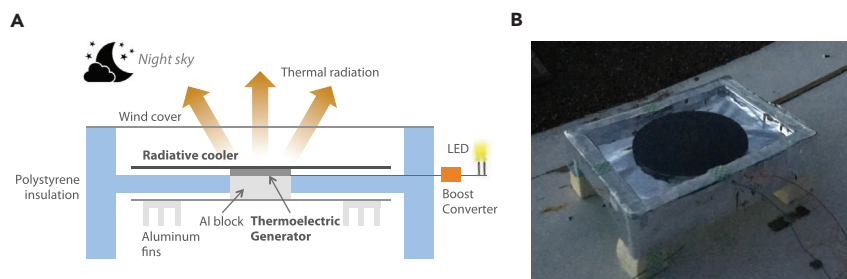


Figure 1. Device Operation Schematic and Picture

(A) Schematic of the low-cost night-time thermoelectric generator device and its key components. (B) Photo of the device in rooftop testing.

We tested performance outdoors on a rooftop in Stanford, CA, USA in late December 2017 under clear-sky conditions with a dew point temperature between -1°C and -3°C during the hours of testing. The device was taken outside shortly after 18:00 h, when the sky was dark. The temperature of the hot and cold sides of the thermoelectric module were monitored with thermocouples (Omega RDXL6SD data logger with an accuracy of $\pm 0.1\%$ or 0.8°C), along with the air temperature immediately next to the finned aluminum disk on the exterior of the enclosure that is near the hot side of the thermoelectric module, which received the heat from the air. The device was exposed to the sky and its power generation capability assessed in regular time intervals by performing a voltage sweep using a high-sensitivity source measure unit (Keithley 2635B).

We show exemplary data from one time point in Figure 2. The voltage sweep shows a short-circuit current $J_{sc} = 44 \text{ mA}$ and an open-circuit voltage $V_{oc} = 79 \text{ mV}$. At the maximum power point, nearly 0.8 mW of power is generated by the thermoelectric module. Normalizing to the area of the radiative cooler this corresponds to 25 mW/m^2 of power generation capacity. In Figure 3, we show the power generated at the maximum power point from the module over 6 h of testing. The fluctuation of the power positively correlates with the fluctuation of the temperature difference between the hot side and cold side. A temperature difference between the two sides of up to 2°C is observed during testing.

To better understand the nature of this performance, we plot the hot and cold side's temperatures along with the measured air temperature in Figure 4A. The radiative cooler, which forms the cold side, is typically 4°C – 5°C below ambient during testing. The hot side of the thermoelectric generator is also a few degrees below ambient. In spite of the presence of natural and forced convection, which has the effect of equalizing the hot side and the ambient temperatures, the conductive heat flow from the hot to the cold side results in the sub-ambient temperature of the hot side.

While the power generated from this demonstration may seem, at first glance, modest, we highlight one application here: lighting. We connect the thermoelectric module to a DC-DC voltage boost converter and a white LED (Jameco 3 mm 8,000 mcd White LED). We note that the boost converter is also passive—it does not take any input besides the input from the thermoelectric generator. As can be seen in Figure 4B, we are able to passively power a LED at night and thus generate light from the cold darkness of space itself. We estimate that the LED was operating at approximately 10% of its maximum brightness.

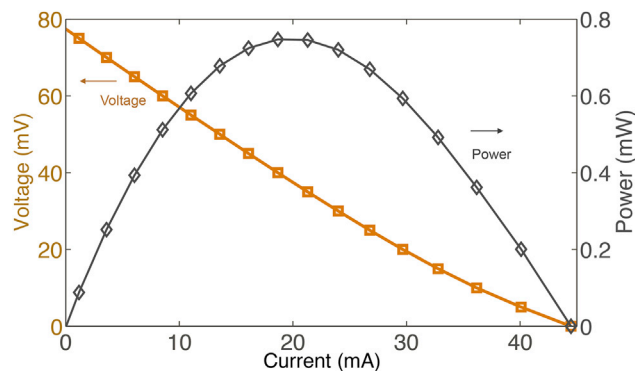


Figure 2. Power Measurement of the Thermoelectric Generator

Current-voltage (I-V) sweep of the device showing an open-circuit voltage (V_{OC}) of nearly 80 mV and a short-circuit current (J_{SC}) of 45 mA, with a max power point value of nearly 0.8 mW.

Theoretical Model

We develop a thermal model to characterize the device's performance in our experiments and to extrapolate potential performance with improved engineering and in varying weather conditions. For this model, the cold side of the thermoelectric module is assumed to be a plate that radiates upward, whose net energy balance we model as:

$$P_{cold}^{net} = P_{rad}(T_c) - P_{atm}(T_{amb}) - P_{convective}(T_c, T_{amb}) - P_{cond} = 0. \quad (\text{Equation 1})$$

In this energy balance, we approximate that the total heat flows are dominated by thermal conduction and neglect heat generation and absorption due to the Seebeck effect and Joule heating in the thermoelectric legs. This simplifying approximation is made since we expect to work in the small temperature-difference regime ($T_h - T_c < 2$ K), where the power conversion efficiency of the thermoelectric module is expected to be well below 0.5%. In Equation 1:

$$P_{rad}(T_c) = A \int d\Omega \cos \theta \int_0^\infty d\lambda I_{BB}(T_c, \lambda) \epsilon(\lambda, \theta), \quad (\text{Equation 2})$$

is the power radiated out by the structure. Here, $\int d\Omega = 2\pi \int_0^{\pi/2} d\theta \sin \theta$ is the angular integral over a hemisphere. $I_{BB}(T, \lambda) = \frac{2hc^2}{\lambda^5} \frac{1}{e^{hc/(\lambda k_B T)} - 1}$ is the spectral radiance of a blackbody at temperature T , where h is Planck's constant, k_B is the Boltzmann constant, c is the speed of light, and λ is the wavelength.

$$P_{atm}(T_{amb}) = A \int d\Omega \cos \theta \int_0^\infty d\lambda I_{BB}(T_{amb}, \lambda) \epsilon_{atm}(\lambda, \theta) \epsilon_{atm}(\lambda, \theta) \quad (\text{Equation 3})$$

is the absorbed power due to incident atmospheric thermal radiation. For simplicity, since our thermal emitter can be approximated as a greybody with average emissivity $\epsilon_s = 0.95$, we can express the above equations as $P_{rad}(T_c) = \epsilon_s \sigma T_c^4$ and $P_{atm}(T_{amb}) = \epsilon_{atm} \epsilon_s \sigma T_{amb}^4$. A previously derived correlation allows us to define the atmospheric emissivity ϵ_{atm} , for a dew point temperature T_{dew} , as $\epsilon_{atm} = 0.741 + 0.0062 \cdot T_{dew}$.⁸ The non-radiative, convective parasitic heat gain to the radiative cooler from its surroundings can be modeled by a coefficient of heat exchange h_{par} :

$$P_{convective}(T_c, T_{amb}) = A \cdot h_{par} (T_{amb} - T_c). \quad (\text{Equation 4})$$

Finally, the heat directly conducted into the radiator through the thermoelectric module from the cold side can be expressed in terms of the net thermal resistance of the thermoelectric module R_{TE} as

$$P_{cond}(T_h, T_c) = A \cdot (T_h - T_c) / R_{TE}. \quad (\text{Equation 5})$$

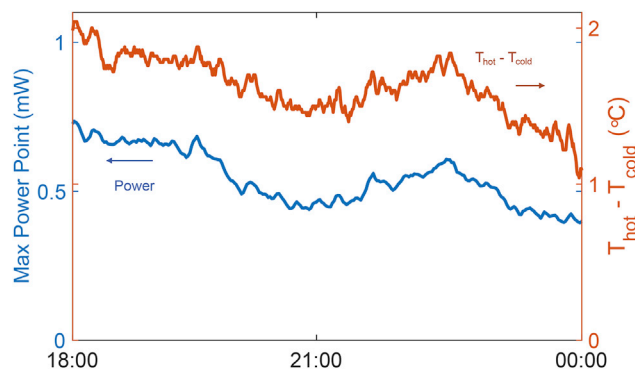


Figure 3. Power Measured over 6 h of Testing

Maximum power point value (blue) in milliwatts as a function of time, along with the temperature difference in degrees Celsius between the hot and cold sides of the thermoelectric generator (red), $\Delta T = T_h - T_c$.

Similarly, we model the net energy flow into the hot side plate of the thermoelectric module, sitting at a temperature of T_h and assumed to have very low emissivity. The hot side can thus be modeled as a simple heat exchanger with its own coefficient of heat exchange with the ambient environment h_{hot} , which is dependent on overall wind patterns and flow behind the fins on the hot-side aluminum plate:

$$P_{hot}^{net}(T_h, T_{amb}) = A \cdot h_{hot}(T_h - T_{amb}) - P_{cond} = 0. \quad (\text{Equation 6})$$

To determine T_c and T_h , we iteratively solve the two equations for the net energy balances P_{cold}^{net} and P_{hot}^{net} , beginning with an initial guess for T_h that is slightly below the ambient air temperature. To evaluate the model's ability to capture our experimentally measured data, we calculate T_h and T_c as a function of time, taking as input our measured air temperature for T_{amb} and the dew point temperature measured from a nearby weather station for T_{dew} , as well as the expected thermal resistance of the thermoelectric (TE) module at this temperature range from the manufacturer, $R_{TE} \approx 2.5$ K/W. Because of varying wind conditions, we evaluate a range of heat exchange coefficient values for both h_{par} and h_{hot} from 7 to 9 W/m²/K. Given the relatively limited insulation provided to the top surface (analogous to the design of Raman et al.¹³ where a similar h_{par} was modeled) and relatively calm wind conditions for the hot side, the fit value range of h_{par} and h_{hot} aligns with expectations. Our model agrees with the experimentally measured temperatures of the hot and cold sides remarkably well, as shown in Figure 5A with the thick bands reflecting the bounds of our model predictions for the range of heat-transfer coefficients modeled for h_{par} and h_{hot} . For the mid-range value of $h_{par} = h_{hot} = 8$ W/m²/K, we evaluate the mean bias error (MBE) and root mean square error (RMSE) of the model's predictions versus the measured values of the temperature difference between the hot and cold sides, $dT = T_h - T_c$. We find that MBE = 0.29°C and RMSE = 0.35°C, errors which are less than 20% of the mean $dT = 1.69$ °C measured during the testing period.

DISCUSSION

Having validated the thermal model, we can use it to predict the temperature difference between the hot and cold sides of the thermoelectric module in different weather conditions as well as through improved thermal engineering. In particular, by suppressing parasitic heat gain in the radiative cooler component to $h_{par} = 0.1$ W/m²/K, improving the heat exchange coefficient of the hot-side to $h_{hot} = 15$ W/m²/K (feasible in windy conditions), we show in Figure 5B that

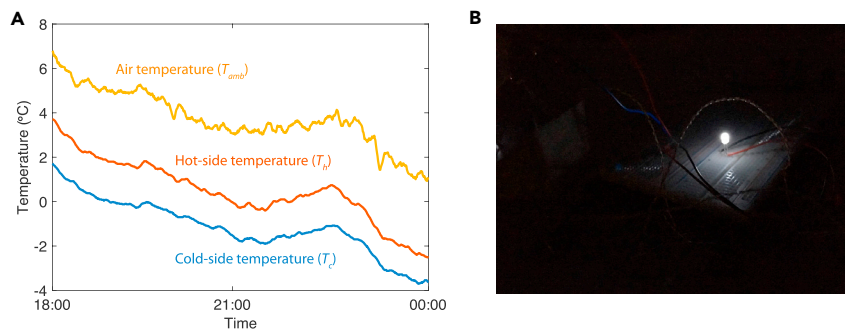


Figure 4. Device Temperatures and LED Operation

(A) Absolute temperature values ($^{\circ}\text{C}$) of the hot and cold sides of the thermoelectric generator along with the ambient temperature.

(B) Picture of the LED operating at night, powered by the radiatively cooled thermoelectric generator.

temperature differences of up to 6.5 K could be achieved with the same thermoelectric module used in testing. This calculated temperature difference can be translated to expected maximum power output under load-matched conditions through an effective model where the maximum power is $W_{\max} = (n\alpha^2(T_h - T_c)^2 / 4R) / A$. For the module used in our experiments, $n = 127$ is the number of thermocouples in the thermoelectric generator, $\alpha = 210.769 \mu\text{V/K}$ is the Seebeck coefficient, $R = 0.007\Omega$ is the resistance per thermocouple, and $A = 0.01\pi\text{m}^2$ is the area of the radiating surface, which we assume to be identical to our experiment (thereby assuming a fixed ratio of the area of the thermoelectric module to radiating surface on the cold side). In favorable conditions, where the ambient air temperature is warm and the dew point low (summer conditions in a Mediterranean or desert climate), we show that power generation of 0.5 W/m^2 may be achievable (Figure 5B).

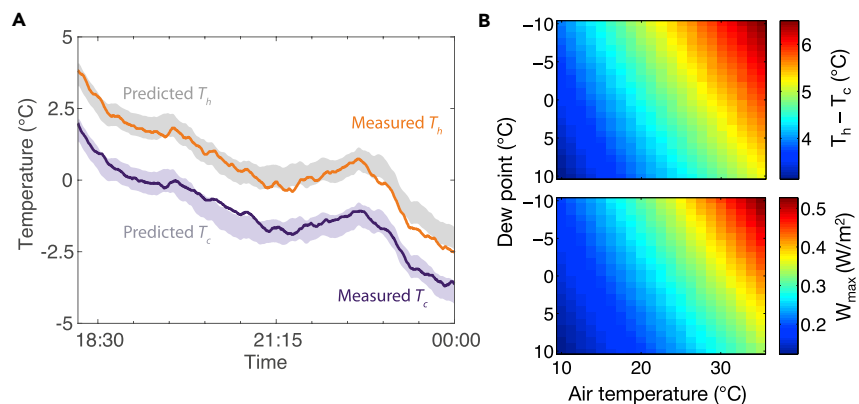


Figure 5. Model Validation and Extrapolation

(A) Comparing the thermal model's prediction for the hot and cold side temperatures (thick light bands) with the experimentally measured temperatures (thin solid lines), we find excellent agreement. The model's boundaries are for parasitic and hot-side convective coefficients of heat exchange h_{par} and h_{hot} varying from 7 to $9 \text{ W/m}^2/\text{K}$, respectively.

(B) Top, the model is extended to predict temperature differences in a range of clear-sky weather conditions as a function of a dew point and air temperature, assuming improved $h_{\text{par}} = 0.1 \text{ W/m}^2/\text{K}$ and $h_{\text{hot}} = 15 \text{ W/m}^2/\text{K}$. A temperature difference between the hot and cold side of nearly 6.5°C is attainable in hot, dry conditions. Bottom, a phenomenological device model for the thermoelectric module used allows us to predict maximum load-matched power output, which may exceed 0.5 W/m^2 in hot, dry conditions.

We emphasize that this result does not represent the ultimate limit of performance for night-time power generation using thermoelectric modules, but is instead intended to point to the practical performance capability of a system similar to the one used here. Another avenue for improved performance is to optimize the area of the radiator relative to the area of the thermoelectric module, as has been done in solar thermoelectric generators.^{28,29} Related to this, we note that the radiative cooling surface used here is black over solar wavelengths, and thus the device tested could function as a solar thermoelectric generator during the day-time. Along with future improvements in the performance of thermoelectric materials and devices designed for low temperature differences, there may be opportunities to reach closer to the limits of power generation through radiative cooling under typical terrestrial atmospheres.²⁶ With increased atmospheric transmittance at higher altitudes or in outer space, the limits of performance will be even higher.²⁷

To summarize, we have highlighted the remarkable possibility and potential of generating small amounts of power by radiative cooling at night using low-cost, off-the-shelf, commodity components (less than \$30 USD for our initial proof of concept demonstration). In off-grid locations throughout the world, this approach of generating light from darkness highlights an entirely new way of maintaining lighting, entirely passively, at night. The power generated could also be used to power small sensors in remote locations, with their lifetimes not being limited by batteries but the lifetime of the thermoelectric module, which can be an order of magnitude longer.³⁰ Unlike other approaches to ambient waste heat recovery using thermoelectric generators, including from human body heat or the mechanical motion of human walking, our strategy is not limited in scale by the human body's dimensions or the area of a particular source of waste heat. In principle, the inherent modularity of this approach allows us to scale the system's size depending on energy needs in a manner similar to photovoltaic systems. As we continue to explore the possibilities emerging from harnessing the cold of space itself for energy applications, our demonstration of direct power generation at night via radiative cooling points to an untapped, yet immediately accessible frontier for both scientific research as well as practical energy generation devices.

ACKNOWLEDGMENTS

This work is supported by the U.S. Department of Energy grant no. DE-FG02-07ER46426, U.S. Department of Energy "Photonics at Thermodynamic Limits" Energy Frontier Research Center under grant no. DE-SC0019140, and the Mellon Family Foundation.

AUTHOR CONTRIBUTIONS

Conceptualization, A.P.R. and S.F.; Methodology, A.P.R.; Investigation, A.P.R. and W.L.; Writing – Original Draft, A.P.R., W.L., and S.F.; Writing – Review & Editing, A.P.R. and S.F.

DECLARATION OF INTERESTS

The authors declare no competing interests.

Received: January 29, 2019

Revised: July 8, 2019

Accepted: August 12, 2019

Published: September 12, 2019

REFERENCES

- Cabraal, R.A., Barnes, D.F., and Agarwal, S.G. (2005). Productive uses of energy for rural development. *Annu. Rev. Environ. Resour.* *30*, 117–144.
- Chaurey, A., Ranganathan, M., and Mohanty, P. (2004). Electricity access for geographically disadvantaged rural communities—technology and policy insights. *Energy Policy* *32*, 1693–1705.
- Deichmann, U., Meisner, C., Murray, S., and Wheeler, D. (2011). The economics of renewable energy expansion in rural sub-Saharan Africa. *Energy Policy* *39*, 215–227.
- Peon, R., Doluweera, G., Platonova, I., Irvine-Halliday, D., and Irvine-Halliday, G. (2005). Solid state lighting for the developing world: the only solution, in: *optics & photonics 2005* (International Society for Optics and Photonics), p. 59410N.
- Catalanotti, S., Cuomo, V., Piro, G., Ruggi, D., Silvestrini, V., and Troise, G. (1975). The radiative cooling of selective surfaces. *Solar Energy* *17*, 83–89.
- Granqvist, C.G., and Hjortsberg, A. (1980). Surfaces for radiative cooling: silicon monoxide films on aluminum. *Appl. Phys. Lett.* *36*, 139–141.
- Granqvist, C.G., and Hjortsberg, A. (1981). Radiative cooling to low temperatures: general considerations and application to selectively emitting sio films. *J. Appl. Phys.* *52*, 4205–4220.
- Berdahl, P., Martin, M., and Sakka, F. (1983). Thermal performance of radiative cooling panels. *Int. J. Heat Mass Transf.* *26*, 871–880.
- Orel, B., Gunde, M.K., and Krainer, A. (1993). Radiative cooling efficiency of white pigmented paints. *Solar Energy* *50*, 477–482.
- Gentle, A.R., and Smith, G.B. (2010). Radiative heat pumping from the earth using surface phonon resonant nanoparticles. *Nano Lett.* *10*, 373–379.
- Rephaeli, E., Raman, A., and Fan, S. (2013). Ultrabroadband photonic structures to achieve high-performance daytime radiative cooling. *Nano Lett.* *13*, 1457–1461.
- Zhu, L., Raman, A., Wang, K.X., Anoma, M.A., and Fan, S. (2014). Radiative cooling of solar cells. *Optica* *1*, 32–38.
- Raman, A.P., Anoma, M.A., Zhu, L., Rephaeli, E., and Fan, S. (2014). Passive radiative cooling below ambient air temperature under direct sunlight. *Nature* *515*, 540–544.
- Zhai, Y., Ma, Y., David, S.N., Zhao, D., Lou, R., Tan, G., Yang, R., and Yin, X. (2017). Scalable-manufactured randomized glass-polymer hybrid metamaterial for daytime radiative cooling. *Science* *355*, 1062–1066.
- Mandal, J., Fu, Y., Overvig, A.C., Jia, M., Sun, K., Shi, N.N., Zhou, H., Xiao, X., Yu, N., and Yang, Y. (2018). Hierarchically porous polymer coatings for highly efficient passive daytime radiative cooling. *Science* *362*, 315–319.
- Vall, S., and Castell, A. (2017). Radiative cooling as low-grade energy source: a literature review. *Renew. Sustain. Energy Rev.* *77*, 803–820.
- Zeyghami, M., Goswami, D.Y., and Stefanakos, E. (2018). A review of clear sky radiative cooling developments and applications in renewable power systems and passive building cooling. *Sol. Energy Mater. Sol. Cells* *178*, 115–128.
- Bagiorgas, H.S., and Mihalakakou, G. (2008). Experimental and theoretical investigation of a nocturnal radiator for space cooling. *Renew. Energy* *33*, 1220–1227.
- Zhang, S., and Niu, J. (2012). Cooling performance of nocturnal radiative cooling combined with microencapsulated phase change material (mpcm) slurry storage. *Energy Build.* *54*, 122–130.
- Goldstein, E.A., Raman, A.P., and Fan, S. (2017). Sub-ambient non-evaporative fluid cooling with the sky. *Nat. Energy* *2*, 17143.
- Vall, S., Castell, A., and Medrano, M. (2018). Energy savings potential of a novel radiative cooling and solar thermal collection concept in buildings for various world climates. *Energy Technol.* *6*, 2200–2209.
- Hu, M., Pei, G., Wang, Q., Li, J., Wang, Y., and Ji, J. (2016). Field test and preliminary analysis of a combined diurnal solar heating and nocturnal radiative cooling system. *Appl. Energy* *179*, 899–908.
- Bell, L.E. (2008). Cooling, heating, generating power, and recovering waste heat with thermoelectric systems. *Science* *321*, 1457–1461.
- Snyder, G.J., and Toberer, E.S. (2008). Complex thermoelectric materials. *Nat. Mater.* *7*, 105–114.
- Heremans, J.P., Jovovic, V., Toberer, E.S., Saramat, A., Kurosaki, K., Charoenphakdee, A., Yamanaka, S., and Snyder, G.J. (2008). Enhancement of thermoelectric efficiency in pbte by distortion of the electronic density of states. *Science* *321*, 554–557.
- Byrnes, S.J., Blanchard, R., and Capasso, F. (2014). Harvesting renewable energy from earth's mid-infrared emissions. *Proc. Natl. Acad. Sci. USA* *111*, 3927–3932.
- Buddhiraju, S., Santhanam, P., and Fan, S. (2018). Thermodynamic limits of energy harvesting from outgoing thermal radiation. *Proc. Natl. Acad. Sci. USA* *115*, E3609–E3615.
- Kraemer, D., Poudel, B., Feng, H.P., Caylor, J.C., Yu, B., Yan, X., Ma, Y., Wang, X., Wang, D., Muto, A., et al. (2011). High-performance flat-panel solar thermoelectric generators with high thermal concentration. *Nat. Mater.* *10*, 532–538.
- Kraemer, D., McEnaney, K., Chiesa, M., and Chen, G. (2012). Modeling and optimization of solar thermoelectric generators for terrestrial applications. *Sol. Energy* *86*, 1338–1350.
- Amatya, R., and Ram, R.J. (2010). Solar thermoelectric generator for micropower applications. *J. Electron. Mater.* *39*, 1735–1740.